Chemical capacitive sensing using ultrathin flexible nanoporous electrodes

Maryna N. Kavalenka[a], Christopher C. Striemer[a,b], Jon-Paul S. DesOrmeaux[b], David Z. Fang[a], Jim L. McGrath[c], Philippe M. Fauchet[a,]

[a] *Electrical and Computer Engineering Department, University of Rochester*
[b] *Simpore Inc.*
[c] *Biomedical Engineering Department, University of Rochester*

Abstract

Ultrathin porous nanocrystalline silicon (pnc-Si) membranes metallized with gold are used as flexible conductive electrodes in chemical capacitive vapor sensor. This use of a porous electrode simplifies the conventional parallel-plate design of typical sensors. Pnc-Si is a 15 nm thick membrane material with pore sizes ranging from 5 to 80 nm and porosities from < 0.1 to 15 % fabricated using standard silicon semiconductor processing techniques. We experimentally test the mechanical stability and elasticity of as prepared pnc-Si and pnc-Si with a conformal metal coating. The very thin porous membrane allows fast analyte vapor permeation to the underlying polymer material that serves as receptor which is tested using an optical profiler. Electrical techniques are used to determine the degree of swelling and the reversibility of the polymer/pnc-Si membrane system when exposed to analyte-containing vapors.

Keywords: porous membrane, capacitive sensor, silicon

1. Introduction

The integration of nanoscale materials into electronic devices such as sensors adds important functionality. Examples include using conductive nanoparticles agglomerates [1, 2] and carbon nanotubes [3, 4] as electrodes in electrical sensor devices to enhance mass transport characteristics [5, 6]. The study of nanopore transport mechanisms [7, 8, 9] and comparisons to ionic channels in the cell membranes have led to interesting chemical and biosensing applications, including single molecule detection [10, 11, 12] and DNA sequencing [13, 14].

In this work we explore the use of a molecularly thin nanoporous membrane material [15] as an analyte-permeable electrode in capacitive sensing [16] to overcome the existing difficulties in making a parallel-plate sensor structure. The use of an ultrathin porous membranes with controllable pore dimensions as a permeable sensor electrode adds the ability for selective access of the analyte molecules to the receptor, and gives control over the mass transport between receptor and sensor environment. The silicon platform also provides for convenient chemical modifications [17]. Transducer elements that convert analyte absorption to electronic signal include capacitance-based transducers that detect changes in dielectric properties [18, 19, 20], resistance-based transducers that monitor changes in resistance [21], and mechanical oscillators that respond to changes in mass [22]. Capacitive sensors are preferred over other transducers because of their high sensitivity, low power and relative ease of fabrication [18, 23, 24].

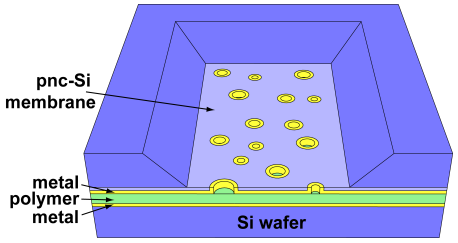

Figure 1: Schematic of the pnc-Si membrane based capacitive sensor

Polymers as receptor materials in capacitive sensors offer low cost, great variety of physical properties and chemical diversity for the selective detection of gas and vapor molecules [25, 26]. The selective absorption of the analyte molecules by the polymer results in reversible swelling or change in electrical properties, altering the sensor capacitance as a function of analyte concentration. Capacitive sensors have two geome-

Email address: fauchet@ece.rochester.edu (Philippe M. Fauchet)

tries: parallel-plate electrodes and interdigitated electrodes (IDE). The parallel-plate sensor has a polymer layer sandwiched between two electrodes. The top electrode in the parallel-plate geometry must be porous for the analyte to reach to the receptor. Etching voids in a top metal layer is challenging because metal etchants can destroy the polymer deposited under metal layer. One solution is to create a parallel-plate MEMs structure with an etched porous electrode on top of the silicon wafer and then infiltrate the polymer later. However this requires sophisticated fabrication steps [18, 27, 28]. The IDE sensor consists of two comb-shaped metal electrodes deposited on a substrate and a sensitive polymer layer deposited on top of them [23, 24, 29]. The IDE sensors are easier to fabricate but they suffer from lower sensitivity because only a fraction of the polymer layer on top of the electrodes contributes to the sensing signal, while the entire polymer layer contributes to the signal sensitivity in parallel-plate sensors.

Here we demonstrate a novel parallel-plate sensor that uses metallized freestanding porous nanocrystalline silicon (pnc-Si) membrane as top electrode. The pnc-Si membranes are 15 nm thick with pore diameters ranging from 5 to 80 nm and porosity from 0.1 to 15 % and are fabricated using standard semiconductor processing techniques [15, 30]. The pores are formed spontaneously during rapid thermal annealing of an amorphous Si layer sandwiched between two SiO_2 layers deposited by RF sputtering. Mechanically strong and flexible pnc-Si membranes are also stable at high temperatures and a wide range of environments [31]. The polymer layer is spin-coated on the metallized membrane and covers the pores. The pore openings serve as nanometer diameter areas available for vapor adsorption. A schematic of the sensor is illustrated in Fig. 1. The metallized pnc-Si membrane forms an ultrathin capacitor plate and the polymer layer serves as the sensing layer.

In this paper we first characterize the mechanical stability and flexibility of pnc-Si membranes at high pressures (>1 atm). We then characterize the reduction in pore diameter and porosity of pnc-Si membranes after metal deposition. The capacitive sensor built using pnc-Si is tested optically and electrically under exposure to different solvent vapors. Finally the capacitance change of the sensor is characterized upon exposure to different concentrations of the same vapor.

2. Materials and Methods

The pnc-Si membrane fabrication procedure is described in detail elsewhere [15, 30]. Briefly, the process starts by growing a thick thermal SiO_2 layer on both sides of a silicon wafer. The backside is then patterned using standard photolithography to create a mask for membrane formation. The front oxide layer is then removed and a three layer film stack (20 nm SiO_2/ 15 nm a-Si/ 20 nm SiO_2) is deposited on the front surface using RF magnetron sputtering. The structure is then treated at high temperature (800 – 1100 °C) in a rapid thermal processing (RTP) chamber. During RTP treatment the amorphous silicon film crystallizes, forming a nanocrystalline film with voids that become the open pores in the membrane. The patterned back side of the wafer is then etched with ethylenediamine pyrocatechol (EDP), which removes the silicon wafer along (111) crystal planes until the first SiO_2 layer of the film stack is reached. Lastly, the three layer membrane is exposed to buffered oxide etchant (BOE) to remove the protective oxide layers, leaving only the freely suspended ultrathin pnc-Si membrane.

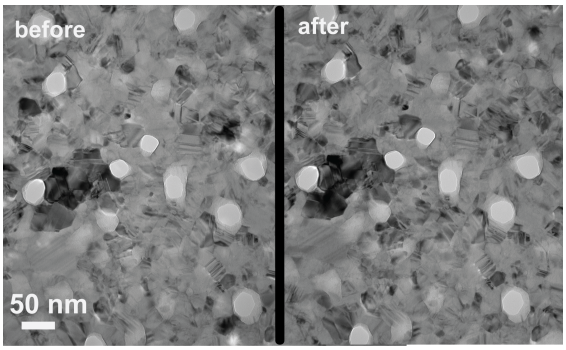

Figure 2: TEM images of the same pnc-Si membrane before and after repeatable stretching at 15 psi. After the imaging, the membrane burst pressure was measured to be 16 psi. The white areas are the open pores, grey is the nanocrystalline silicon and the darker areas in the image are nanocrystals with crystal plane alignment satisfying the Bragg condition.

The metallization of pnc-Si with gold (Au) was performed by e-beam evaporation in a CHA e-beam evaporator at base pressures $\sim 10^{-7}$ Torr. A 3-10 nm layer of titanium (Ti) was deposited first, as adhesion of gold to silicon is poor and requires an adhesion layer [32]. The 10-15 nm gold layer was deposited next in the same run without vacuum breaking to prevent Ti layer oxidation. The deposition rates of Au and Ti are 0.5-1 Å/s and 1-4 Å/s correspondingly. Deposition rates and film thicknesses were measured by the frequency shift of a quartz crystal microbalance. The metallized pnc-Si membranes used in capacitive sensor measurements have < 1% and ~ 2% porosities.

Transmission electron microscopy (TEM) images

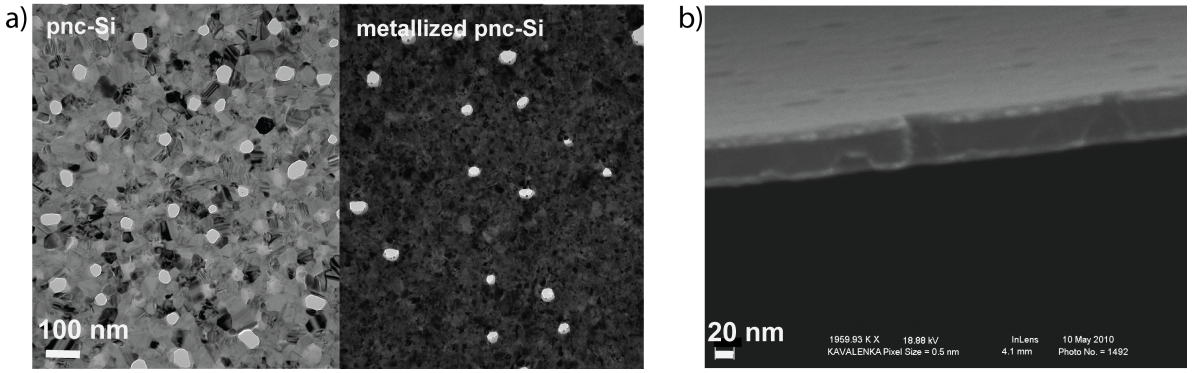

Figure 3: a) TEM images of the same 15 nm thick pnc-Si membrane before and after metallization with 15 nm layer of gold; b) SEM of the crossection of the 30 nm thick pnc-Si membrane with approximately 15-20 nm gold layer deposited on each side.

were obtained using a Hitachi 7650 Transmission Electron Microscope. Scanning electron microscope (SEM) studies of the metallized membranes were done using a Zeiss Supra 40VP. Optical measurements of the sensor response to vapor introduction were done using Veeco Wyko optical profiler.

Sensor fabrication began with metal deposition on top of both the pnc-Si membrane and the silicon wafer chip, followed by polymer deposition [16]. The polydimethylsioloxane (PDMS) Sylgard 184 from Dow Corning is a convenient and widely available polymer. The elastomer was first mixed with its curing agent in 10:1 ratio and then placed in a desiccator to remove the bubbles created while mixing. The PDMS layer was created by spin-coating the mixture on silicon at 4000-6000 rpm for 1-4 min. The thickness of the resulting PDMS layer ranged form 5 to 10 μm depending on the spin rate and duration. The pnc-Si chip and PDMS covered silicon chip were then bonded together and cured at 95 °C for 2 hours to form sensor as in Fig. 1. Following fabrication, conductive silver epoxy was used to adhere wire connections to the sensor electrodes.

A HP4275A multifrequency LCR meter controlled by Labview was used to measure the capacitance of the completed sensor. The sensor capacitance was continuously sampled using a National Instruments GPIB-USB interface. All measurements were done in the parallel capacitive mode, with an AC signal of 10 kHz and voltage amplitude of 100 mV. The sensor chip was connected to the LCR meter with the backside well facing up to ensure vapor permeation through the porous membrane. The sensors were then placed in a sealed 3.8 L glass container. Real-time data was collected during solvent introduction. A pipette was used to inject a known concentration (parts per million, ppm) of liquid solvent (hexane, toluene, acetone, xylene) into the glass container and was let to evaporate. An immediate change in capacitance was observed. The sensor was then taken out or flushed with air for few minutes to allow the capacitance to regain its original value, and then exposed to solvent vapor again. This procedure was repeated several times.

3. Results and Discussion

3.1. Mechanical stability of pnc-Si

Mechanical stability and flexibility are important electrode properties for swelling-induced sensors. Using a custom pressure cell to seal pnc-Si membranes with an O-ring [9], we tested the burst pressure of the pnc-Si membranes. Nitrogen was used to pressurize the system upstream of the membrane and a manometer monitored the increasing gauge pressure throughout the experiment. The average burst pressures of pnc-Si membranes strongly depended on the fabrication conditions. The measured average burst pressures range was from few psi up to 25 psi.

As previously reported by our group pnc-Si membranes elastically and reversibly deform when pressurized [15]. To confirm this result at the nanoscale level, we applied pressures just below the burst pressure across pnc-Si for 30 min, and examined the membranes by TEM. TEM micrographs taken on the same area before and after repeated stretching under 15 psi are illustrated in Fig. 2. As seen in the TEM images the positions of the nanocrystals and the pores is unchanged.

3.2. Pnc-Si after metallization

TEM images of a pnc-Si membrane before and after metallization are shown in Fig. 3a. They demonstrate that pores have not been occluded after Ti/Au bilayer

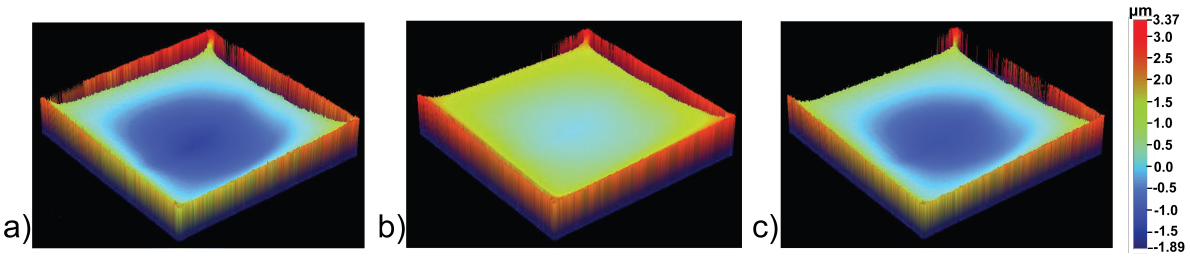

Figure 4: 3D optical profilometry images of a pnc-Si/PDMS/Si structure: a) before exposure to vapor; b) immediately after exposure to xylene vapor; c) approximately 2 minutes after the vapor is removed. The wall-like area around the membrane window is an artifact of the imaging as the optical profiler picks up the signal reflected not only from the square membrane area but also from the walls of the silicon well which was etched to expose the freestanding pnc-Si membrane.

film deposition. The nearly circular white areas are the open pores in both images. Deposition of the metal layer on pnc-Si membrane closed small pores and reduced the diameters of the larger pores. For example, deposition of a 13 nm metal bilayer on two different 15 nm thick pnc-Si membranes caused the porosity to drop from 4.8 to 3.3 % and from 13.4 to 6.2 %. The corresponding average pore size reductions were from 19 nm to 15.5 nm and from 28 nm to 23 nm. The porosity and pore distribution of pnc-Si membranes changed with the deposited metal thickness. The SEM image of the cross section of the 30 nm thick pnc-Si membrane metallized on both sides shown in Fig. 3b illustrates the conformal coating of the pores.

3.3. Pnc-Si deflection during PDMS swelling

Because the pnc-Si membranes are very thin, their resistance to flow is very small [8, 9]. To determine if the analyte vapor above the membrane permeated through the membrane to reach the polymer beneath it, we conducted an experiment on the pnc-Si/PDMS/Si wafer structure to monitor reversible changes is the PDMS thickness in xylene vapor [16] . The sensor was exposed to xylene vapor and the change in the surface height before and after exposure was measured. Optical profilometry was used to measure the induced swelling. In this interferometric technique white light first passes through a beam splitter and is directed to the sample surface and a reference mirror. Reflected light from both surfaces is later recombined to produce an interference fringe pattern which gives information about the surface contour of the sample [33].

The deflection of a pnc-Si/PDMS/Si structure was observed before, during and after exposure to xylene vapor. The 3D optical profilometry images of the structure taken from the well-side of the pnc-Si membrane are shown in Fig. 4. The square window area in these images is the pnc-Si membrane covering the PDMS layer. The surface height is represented by the color scale. Xylene vapor permeation through the pores induced PDMS swelling under the pnc-Si membrane. A 0.38 μm increase in thickness of the initial PDMS layer was measured when vapor was introduced into the system. The swelling was reversible: after the vapor source was removed the membrane came back to its initial state as shown in Fig. 4c.

3.4. Chemical capacitive sensing

The sensing principle of a capacitive sensor is based on the capacitance relationship of a parallel-plate capacitor which is $C = \epsilon_0 \epsilon_r A/d$, where ϵ_0 is the permittivity of vacuum, ϵ_r is relative dielectric constant of the dielectric layer, A is the overlap area between two plates, and d is the separation between plates. The capacitance changes in response to changes in ϵ_r or d. The effects of polymer swelling ($d + \Delta d$) and change of dielectric constant ($\epsilon_r + \Delta\epsilon_r$) may cancel each other. To maximize the capacitive response the polymer and solvent were chosen so that one of these mechanisms is dominant. Test solvents, including hexane, toluene, and acetone, were selected for this experiment as they are readily available, quick to evaporate and induce only one of these two changes in PDMS. For hexane and toluene the polymer swelling dominates, while for acetone vapor the dielectric constant change dominates [34].

The experimental capacitance data upon exposure of the same sensor to different vapors is shown in Fig. 5. The sensor was repeatedly exposed to hexane and then toluene vapor at the 800 ppm and 1000 ppm levels respectively. During exposures sensor capacitance was allowed to reach stable value. Between exposures the sensor was removed from the container and allowed to recover. Both solvents swelled PDMS leading to an increase in plate separation and capacitance decrease. Hexane swells PDMS more than toluene, which is expected given their different solubility parameters δ

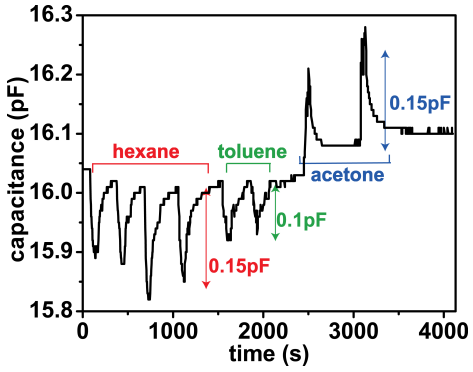

Figure 5: Capacitive response of the sensor upon exposure to hexane, toluene and acetone vapors.

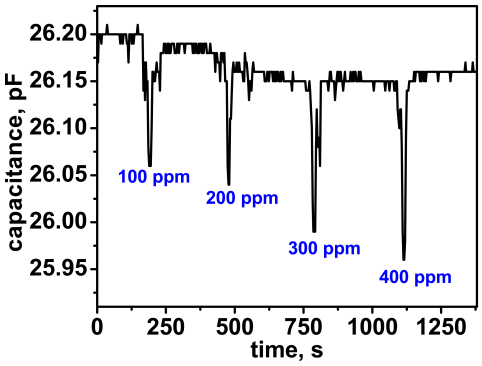

Figure 6: Capacitive response of the sensor upon exposure to controlled xylene concentrations.

($\delta_{PDMS} = \delta_{hexane} < \delta_{toluene}$) [34]. The ϵ_r of hexane and toluene are close to that of PDMS and so net change in ϵ_r is negligible. The measured changes in capacitance induced by hexane and toluene were 0.15 pF and 0.1 pF, respectively. Next the sensor was exposed to acetone vapor. For acetone ϵ_r is much higher than for PDMS ($\epsilon_{racetone} > \epsilon_{rPDMS}$) resulting in an increase of the sensor capacitance by 0.15 pF upon acetone exposure. By contrast PDMS swelling induced by acetone is negligible [34].

Fig. 6 shows a typical sensor response upon exposure to different xylene vapor concentrations (100, 200, 300, 400 ppm). After each exposure the sensor was brought to its original value by passing air. The response and recovery times of the sensor are functions of pore size and porosity, and decrease with increasing pores size, as bigger pores facilitate vapor molecules diffusion into and out of the sensor [35].

4. Conclusions

We have demonstrated a new approach to the fabrication of an electrical sensor for organic vapor detection employing ultrathin flexible pnc-Si membrane as a porous electrode. Using a porous electrode simplifies the fabrication of conventional capacitive parallel-plate sensors traditionally constructed with etch-through electrodes. The mechanical strength and elasticity of pnc-Si were tested and no measurable plastic deformation was observed. Devices were built and sucessfully operated in solvent vapor enviroments. The swelling caused by vapor permeation was measured by optical profilometry. Reversible real-time capacitance response of the sensor was obtained for three solvents that use different mechanisms for capacitance changes, as well as for different concentrations of the same vapor. Since both membrane and sensor fabrication are compatible with standard microfabrication processes, ultimately multiple sensors could be integrated on a single silicon chip.

Acknowledgements

We acknowledge the National Science Foundation for support of this work under grants CBET0707795 and ECCS0707795. Device fabrication and characterization was performed at the University of Rochester Nanosystems Center and Rochester Institute of Technology Semiconductor Microfabrication Facility.

References

[1] E. Dovgolevsky, U. Tisch, H. Haick, Chemically sensitive resistors based on monolayer-capped cubic nanoparticles: towards configurable nanoporous sensors, Small 5 (2009) 1158.
[2] A. Tricoli, S. E. Pratsinis, Dispersed nanoelectrode devices, Nat. Nanotechnol. 5 (2010) 54.
[3] Y. Lin, F. Lu, Y. Tu, Z. Ren, Glucose biosensors based on carbon nanotube nanoelectrode ensembles, Nano Lett. 4 (2004) 190.
[4] T. J. Kang, M. Cha, E. Y. Jang, J. Shin, H. U. Im, Y. Kim, J. Lee, Y. H. Kim, Ultra-thin and conductive nanomembrane arrays for nanomechanical transducers, Adv. Mater. 20 (2008) 3131.
[5] G. S. Attard, P. N. Bartlett, N. R. B. Coleman, J. M. Elliott, J. R. Owen, J. H. Wang, Mesoporous platinum films from lyotropic liquid crystalline phases.
[6] D. W. M. Arrigan, Nanoelectrodes, nanoelectrode arrays and their applications, Analyst 129 (2004) 1157.
[7] H. D. Tong, H. V. Jansen, V. J. Gadgil, C. G. Bostan, C. G. E. Berenschot, C. J. M. van Rijn, M. Elwenspoek, Silicon nitride nanosieve membrane.
[8] T. R. Gaborski, J. L. Snyder, C. C. Striemer, D. Z. Fang, M. Hoffman, P. M. Fauchet, J. McGrath, ACS Nano 4 (2010) 6973.
[9] M. N. Kavalenka, C. C. Striemer, D. Z. Fang, T. R. Gaborski, J. L. McGrath, P. M. Fauchet, Ballistic and non-ballistic flow through ultrathin nanopores, Small (submitted) (2011).

[10] C. Dekker, Solid-state nanopores, Nat. Nanotechnol. 2 (2007) 209.
[11] R. M. M. Smeets, S. W. Kowalczyk, A. R. Hall, N. H. Dekker, C. Dekker, Translocation of reca-coated double-stranded dna through solid-state nanopores, Nano Lett. 9 (2009) 3089.
[12] R. Wei, D. Pedone, A.Zurner, M. Doblinger, U. Rant, Fabrication of metallized nanopores in silicon nitride membranes for single-molecule sensing, Small 6 (2010) 1406.
[13] A. Singer, M. Wanunu, W. Morrison, H. Kuhn, M. D. Frank-Kamenetskii, A. Meller, Nanopore based sequence specific detection of duplex dna for genomic profiling, Nano Lett. 10 (2010) 738.
[14] E. C. Yusko, J. M. Johnson, S. Majd, P. Prangkio, R. C. Rollings, J. Li, J. Yang, M. Mayer, Controlling protein translocation through nanopores with bio-inspired fluid walls, Nature 6 (2011) 253.
[15] C. C. Striemer, T. R. Gaborski, J. L. McGrath, P. M. Fauchet, Charge- and size-based separation of macromolecules using ultrathin silicon membranes, Nature 445 (2007) 749.
[16] M. N. Kavalenka, C. C. Striemer, D. Z. Fang, T. R. Gaborski, J. L. McGrath, P. M. Fauchet, Hybrid polymer/ultrathin porous nanocrystalline silicon membranes system for flow-through chemical vapor and gas detection, Active polymers, Mater. Res. Soc. Symp. Proc., San Francisco, CA, 2009 1190.
[17] D. Z. Fang, C. C. Striemer, T. R. Gaborski, J. L. McGrath, P. M. Fauchet, Nano Lett. 10 (2010) 3904.
[18] S. V. Patel, T. E. Mlsna, B. Fruhberger, E. Klaassen, S. Cemalovic, D. R. Baselt, Chemicapacitive microsensors for volatile organic compound detection, Sens. Actuators B 96 (2003) 541.
[19] S. Satyanarayana, D. T. McCormick, A. Majumdar, Parylene micro membrane capacitive sensor array for chemical and biological sensing, Sens. Actuators B 115 (2006) 494.
[20] K. K. Park, H. J. Lee, G. G. Yaralioglu, A. S. Ergun, O. Oralkan, M. Kupnik, C. F. Quate, B. T. Khuri-Yakub, T. Braun, J.-P. Ramseyer, H. P. Lang, M. Hegner, C. Gerber, J. K. Gimzewski, Capacitive micromachined ultrasonic transducers for chemical detection in nitrogen, Appl. Phys. Lett. 91 (2007) 094102.
[21] J. R. Li, J. R. Xu, M. Q. Zhang, M. Z. Rong, Carbon black/polystyrene composites as candidates for gas sensing materials, Carbon 41 (2003) 2353.
[22] J. D. Adams, G. Parrott, C. Bauer, T. Sant, L. Manning, M. Jones, B. Rogers, D. McCorkle, T. L. Ferrell, Nanowatt chemical vapor detection wit a self-sensing, piezoelectric microcantilever array, Appl. Phys. Lett. 83 (2003) 3428.
[23] M. Kitsara, D. Goustouridis, S. Chatzandroulis, M. Chatzichristidi, I. Raptis, T. Ganetsos, R. Igreja, C. J. Dias, Single chip interdigitated electrode capacitive chemical sensor arrays, Sens. Actuators B 127 (2007) 186.
[24] A. M. Kummer, A. Hierlemann, H. Baltes, Tuning sensitivity and selectivity of complementary metal oxide semiconductor-based capacitive chemical microsensors, Anal. Chem 76 (2004) 2470.
[25] B. Adhikari, S. Majumdar, Polymers in sensor applications, Prog. Polym. Sci. 29 (2004) 699.
[26] M. A. C. Stuart, W. S. Huck, J. Genzer, M. Muller, C. Ober, M. Stamm, G. B. Sukhorukov, I. Szleifer, V. V. Tsukruk, M. Urban, F. Winnik, S. Zauscher, I. Luzinov, S. Minko, Emerging applications of stimuli-responsive polymer materials, Nat. Mat. 9 (2010) 101.
[27] S. V. Patel, S. T. Hobson, S. Cemalovic, T. E. Mlsna, Detection of methyl salicylate using polymer-filled chemicapacitors, Talanta 76 (2008) 872.
[28] D. L. McCorkle, R. J. Warmack, S. V. Patel, T. Mlsna, S. R. Hunter, T. L. Ferrell, Ethanol vapor detection in aqueous environments using micro-capacitors and dielectric polymers, Sens. Actuators B 107 (2005) 892.
[29] A. Hierlemann, D. Lange, C. Hagleitner, N. Kerness, A. Koll, O. Brand, H. Baltes, Application-specific sensor systems based on cmos chemical microsensors, Sens. Actuators B 70 (2000) 2.
[30] D. Z. Fang, C. C. Striemer, T. R. Gaborski, J. L. McGrath, P. M. Fauchet, J. Phys.: Condens. Matter 22 (2010) 454134.
[31] A. A. Agrawal, B. J. Nehilla, K. V. Reisig, T. R. Gaborski, D. Z. Fang, C. C. Striemer, P. M. Fauchet, J. L. McGrath, Porous nanocrystalline silicon membranes as highly permeable and molecularly thin substrates for cell culture.
[32] A. A. R. Elshabini-Riad, F. D. Barlow, Thin Film Technology Handbook, McGraw-Hill, 1997.
[33] W. Osten, Optical inspection of microsystems, CRC Press, 2007.
[34] J. N. Lee, C. Park, G. M. Whitesides, Solvent compatibility of poly(dimethylsiloxane)-based microfluidic devices, An. Chem. 75 (2003) 6544.
[35] E. C. Dickey, O. K. Varghese, K. G. Ong, D. Gong, M. Paulose, C. A. Grimes, Room temperature ammonia and humidity sensing using highly ordered nanoporous alumina films, Sensors 2 (2002) 91.